

## Flow around four circular cylinders in square configuration

X.K. Wang and S.K. Tan

Maritime Research Centre  
 Nanyang Technological University, 50 Nanyang Avenue, 639798, Singapore

### Abstract

This paper presents an experimental study on four circular cylinders of equal diameters arranged in the in-line square configuration and subjected to a cross-flow. With the cylinder diameter  $D$  and free-stream velocity  $U$  kept constant (resulting in a fixed Reynolds number of  $Re = 1.1 \times 10^4$ ), the present work aims to investigate the effects of varying the cylinders' centre-to-centre pitch (or spacing) on the flow patterns around the four-cylinder array as well as the hydrodynamic forces (lift and drag) on each cylinder. Five pitch ratios ( $P/D$ ) varying from 2.0 to 4.0 have been studied. The flow fields are measured using a digital Particle Image Velocimetry (PIV) system. At the same time, the hydrodynamic forces (drag and lift) on each cylinder have been directly measured using a Piezoelectric load cell.

### Introduction

The study of flow around circular cylindrical structures is of both fundamental and practical significance. As a result, a great deal of research work has been carried out in order to understand the classical problem of an isolated, single circular cylinder in cross flow. On the other hand, in many cases, cylindrical structures are stacked in groups (or arrays) in the design of offshore structures, chimneys, power lines, heat exchangers tubes, etc. Due to mutual interference between the cylinders in proximity to each other, the flow usually shows a much more complicated behaviour, and thus is less well studied and understood than the case of a single cylinder. It is thus desirable to investigate the flow passing through multiple-cylinder arrays.

Due to the presence of neighbouring cylinders, the flow pattern, force coefficients, vortex shedding, and vortex-induced vibration (VIV) of each cylinder would significantly vary. The interference between two cylinders arranged in tandem, side-by-side, or staggered configurations, being the simplest example of an array of cylinders, have drawn considerable attention over the last two decades, see a recent review by Sumner [11] on this topic which includes more than 130 papers in the literature. Most of the previous studies considered the two-dimensional (2D) case, and it is established that three most important variables governing the flow behaviour are: (i) the spacing between the cylinders (which is typically expressed as the ratio between the centre-to-centre pitch and the cylinder diameter,  $P/D$ , thereafter abbreviated as the pitch ratio); (ii) the angle of incidence for the cylinder array relative to the free stream ( $\alpha$ ); and (iii) the Reynolds number ( $Re$ ), which is defined as  $Re = UD/\nu$ , where  $U$  is the free-stream velocity and  $\nu$  is the kinematic viscosity.

A four-cylinder array in the square configuration, which is shown in Figure 1, is a fundamental element in offshore structures (e.g., semi-submersible platform), pipe bundles and tube banks. Due to the flow complexity, however, there are only a handful of studies on this configuration. The four-cylinder array arranged in the

square configuration was first investigated by Sayers [9, 10] on the force coefficients and vortex shedding frequencies at  $Re = 3 \times 10^4$  under different pitch ratios and incident angles. The present understanding of this flow configuration was largely attributed to the long-term research by Lam and co-authors over the past 20 years [e.g., 2–8, 13, 14].

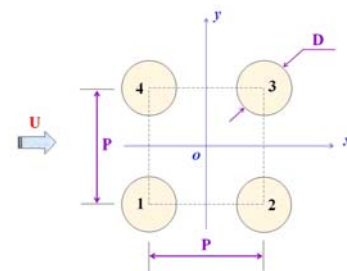


Figure 1. Schematic of the four-cylinder array in the in-line configuration and coordinate system.

It is noted that nearly all the prior experiments were conducted either at laminar regime ( $Re = 100 - 200$ , mainly for flow visualization study) or subcritical regime ( $Re = 10^3 - 10^4$ , for measurement of pressure, drag/lift forces, velocity). There are also several numerical studies available in the literature. Except for the LES study by Lam and Zou [6, 7] and Zou et al. [13] at  $Re = 1.5 \times 10^4$ , the rest numerical studies are restricted to relatively low Reynolds numbers  $Re < 300$  [2, 8, 14]. The review indicates that while the flow is somewhat sensitive to  $Re$ , it strongly depends on the pitch ratio ( $P/D$ ). Lam and Lo [5] classified the flow pattern into three distinct regimes as a function of  $P/D$ : namely, the shielding, reattachment and impinging regimes, as shown in Figure 2. Because of the complicated flow interference, the vortex shedding frequency ( $f$ ), always expressed in non-dimensional form as the Strouhal number,  $St = fD/U$ , varies significantly across the wake. The different vortex shedding frequencies would be appropriately associated with individual shear layers rather than the individual cylinders, as suggested by Sumner et al. [12] on two cylinders in staggered arrangement. The extensive investigations by Lam and co-authors [1, 3, 4, 6, 7, 13] at different Reynolds numbers confirmed the distinct flow regimes (though the exact values of  $P/D$  to delineate the flow regimes may vary among those studies), as well as the corresponding change in the force coefficients and vortex shedding frequencies [1, 4].

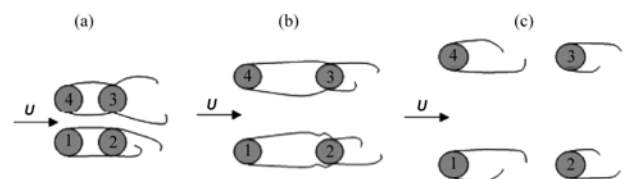


Figure 2. Typical flow patterns around four cylinders in an in-line square configuration: (a) shielding; (b) reattachment; and (c) impinging. Adapted from [2].

Nevertheless, due to the limited experimental data from the previous studies, a number of important issues have yet to be clarified on flow interference between the four cylinders in square configuration and also on each cylinder. For instance, most of the previous studies obtained the force coefficients by integrating the pressure distribution on the cylinder surface at mid-span [1, 9, 10]. The only study in the literature that directly measured the spanwise averaged forces is [4], in which, however, only one cylinder of the four-cylinder array was instrumented with a load cell, and hence a simultaneous measurement of the forces on the four cylinders is not available.

## Experimental Setup and Methodology

The experiments were performed in the re-circulating rectangular open channel located at Maritime Research Centre, Nanyang Technological University, with a test section of  $5 \text{ m} \times 0.3 \text{ m} \times 0.45 \text{ m}$  (length  $\times$  width  $\times$  height). The flow velocity in the test section could be set to a value between 0.02 and 0.7 m/s. The free-stream velocity was uniform to within 1.5% across the test section, and the turbulence intensity in the free stream was well below 2%. The cylinder models, made of smooth, transparent, acrylic rod with an outer diameter of  $D = 20 \text{ mm}$ , were suspended vertically in the water channel and subjected to the cross flow. During the experiments, the free-stream velocity was kept constant at  $U = 0.55 \text{ m/s}$  ( $Re = 1.1 \times 10^4$ ). As shown in Figure 1, the origin of the coordinate system is located at the centre point of the four cylinder, with  $x$ ,  $y$  and  $z$  denoting the streamwise, transverse and spanwise directions, respectively. The cylinders' centre-to-centre pitch was varied, resulting in the pitch ratio to be  $P/D = 2.0, 2.5, 3.0, 3.5$  and  $4.0$ . The blockage ratio per cylinder was about 6.7%, which is similar to that in [3, 4, 7]. During the experiments, the water depth was kept constant at  $H = 200 \text{ mm}$ . This led to an aspect ratio of 10, which is considered to be large enough to ensure the flow to be nominally 2-dimensional (2D) in the near wake. Thus, all the PIV measurements were carried out at the horizontal, mid-span plane of the submerged part of the cylinders.

A LaVision PIV system was used. The flow field was illuminated with a double cavity Nd:YAG laser light sheet at 532 nm wavelength (Litron model, power  $\sim 135 \text{ mJ}$  per pulse, duration  $\sim 5 \text{ ns}$ ). Spherichel<sup>®</sup> 110P8 hollow glass spheres (neutrally buoyant with a mean diameter of  $13 \mu\text{m}$ ) were seeded in the flow as tracer particles, which offered good traceability and scattering efficiency. The images were recorded using a 12-bit CCD camera, which had a resolution of  $1600 \times 1200$  pixels. Particle displacement was calculated using the fast-Fourier-transform (FFT) based cross-correlation algorithm with standard Gaussian sub-pixel fit structured as an iterative multi-grid method. The processing procedure included two passes, starting with a grid size of  $64 \times 64$  pixels, stepping down to  $32 \times 32$  pixels overlapping by 50%, which resulted in a set of 7500 vectors ( $100 \times 75$ ) for a typical field. In between passes, the vector maps were filtered by using a  $3 \times 3$  median filter in order to remove possible outliers. The final vector maps were smoothed with a  $3 \times 3$  average filter. The field of view was  $200 \text{ mm} \times 150 \text{ mm}$  ( $L \times W$ ), therefore the spatial resolution for the present setup was  $2 \text{ mm} \times 2 \text{ mm}$  (i.e.,  $0.1D \times 0.1D$ ). For each case, a series of 840 instantaneous flow fields were acquired at the sampling frequency of 15 Hz (or 56s recordings). The uncertainty in the instantaneous velocities ( $u$  and  $v$ ) was estimated to be about 2%. Based on the velocity vector distribution, the instantaneous spanwise vorticity ( $\omega_z = \Delta v / \Delta x - \Delta u / \Delta y$ ) was calculated using the least squares extrapolation scheme. The uncertainty in  $\omega_z$  was about 10%.

A load cell (3-component piezoelectric Kistler Model 9317B) was mounted between each cylinder and the mounting plate to directly measure the hydrodynamic forces, drag ( $F_D$ ) and lift ( $F_L$ ), on the cylinder (integrated over the immersed span of the cylinder). The amplified output was captured with a National Instruments D/A card at a sampling rate of 1000 Hz. The duration of each recording was about 200 s. Then, the mean and RMS values of drag and lift coefficients of each cylinder were calculated. Through a number of repeated measurements on a stationary cylinder, the uncertainty in the mean drag coefficient ( $\bar{C}_D$ ) was determined to be within 1%.

## Results and Discussion

Figure 3 shows the variation of measured lift and drag coefficients of each cylinder with respect to  $P/D$ .

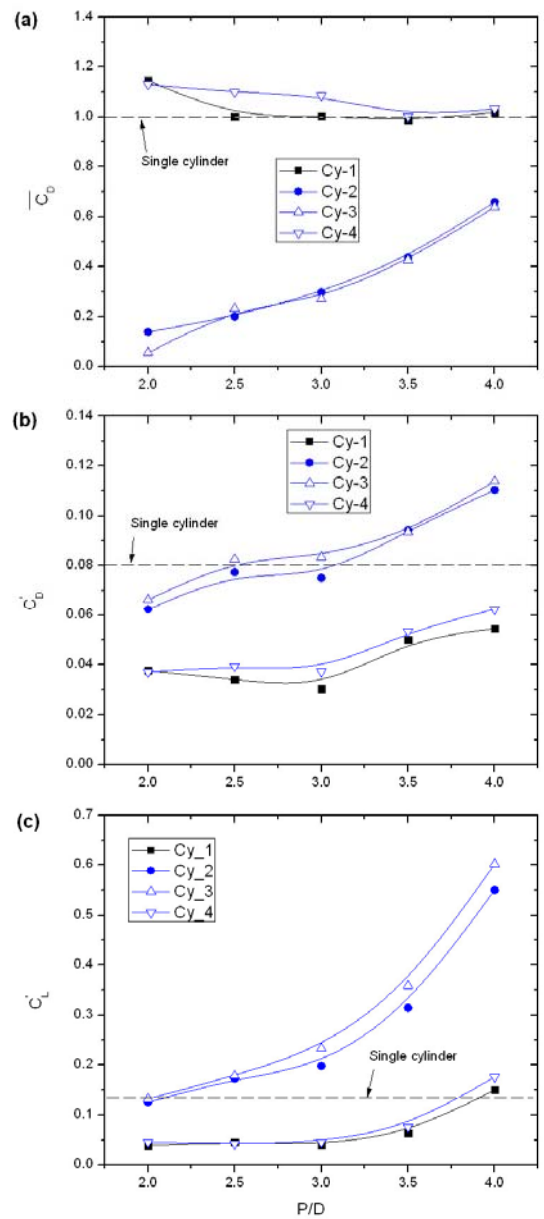


Figure 3. Variation of hydrodynamic coefficients as a function of  $P/D$ : (a) Mean drag coefficient ( $\bar{C}_D$ ); (b) RMS drag coefficient ( $C'_D$ ); and (c) RMS lift coefficient ( $C'_L$ ).

Generally the force coefficients of the two upstream cylinders (Cy-1 and Cy-4), as well as those of the two downstream cylinder (Cy-2 and Cy-3), are almost the same due to the flow symmetry about  $x$ -axis. Immersed in the wake of the upstream cylinders, the downstream cylinders always have a lower drag force. While  $\overline{C_D}$  for Cy-2 and Cy-3 increases monotonically with  $P/D$  within the measurement range, that for Cy-1 and Cy-4 slightly decreases over the small  $P/D$  range ( $P/D \leq 2.5$ ) and thereafter keeps almost constant at a value which is roughly the same as that of an isolated, single cylinder, i.e.,  $\overline{C_D} \approx 1.0$ . The RMS coefficients,  $C'_D$  and  $C'_L$ , of each cylinder, however, increase monotonically with increasing  $P/D$ . The magnitude of  $C'_D$  and  $C'_L$  for the two downstream cylinders (Cy-2 and Cy-3) can be several times higher than that of the upstream ones (Cy-1 and Cy-4), due to the interference of the shear layers separated from the upstream cylinders with the downstream cylinders. A sharp increase in both  $C'_D$  and  $C'_L$  occurs after  $P/D \approx 3.5$  and beyond, which corresponds to the transition of flow pattern from the shear layer reattachment pattern to the periodic vortex impinging pattern, as will be illustrated by the PIV results.

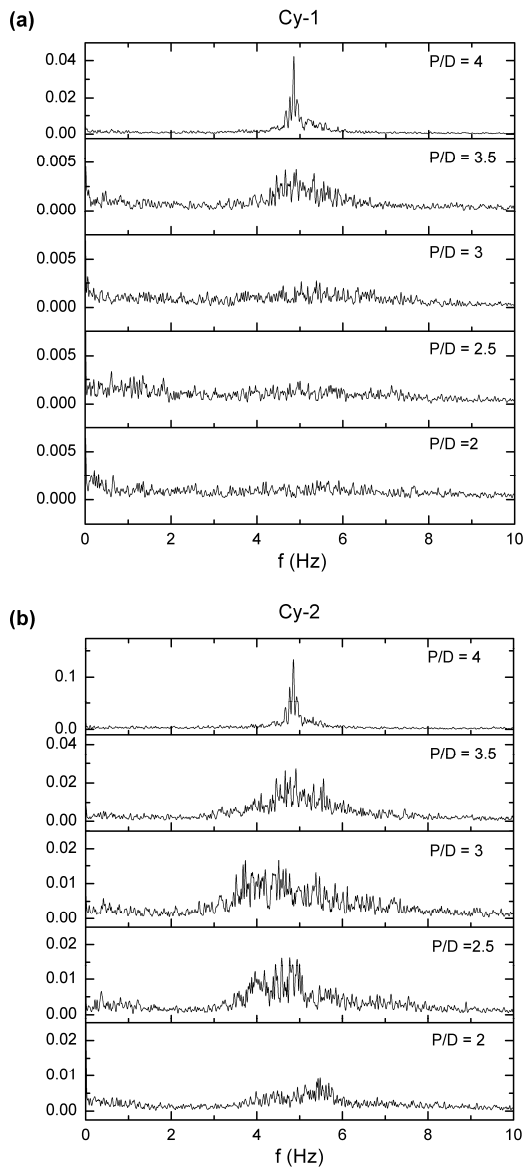


Figure 4. Amplitude spectrum of fluctuating lift force at different pitch ratios for: (a) Cy-1; and (b) Cy-2.

The vortex shedding frequencies can be estimated from the power spectrum of the fluctuating lift force. Figure 4 shows the power density function of the lift forces on Cy-1 (upstream) and Cy-2 (downstream) at different pitch ratios. For Cy-1, a prominent peak at  $f = 4.9$  Hz is observed in the spectrum for  $P/D \geq 4.0$ , but when  $P/D < 3.5$ , there are no obvious peaks. For Cy-2, on the other hand, apparent peaks can be found even at the smallest pitch ratio of  $P/D = 2.0$ . It should be noted that, however, at moderate pitch ratios ( $2.5 \leq P/D \leq 3.5$ ), more than one peaks are observed in the spectrum, indicating that the interference of the shear layers from the upstream cylinders with the downstream cylinders is complex, which may involve intermittent reattachment. When the pitch ratio is even larger ( $P/D \geq 4.0$ ), the peak becomes sharp and dominant, suggesting occurrence of mature vortex shedding from the upper cylinders and subsequent impinging on the downstream cylinder.

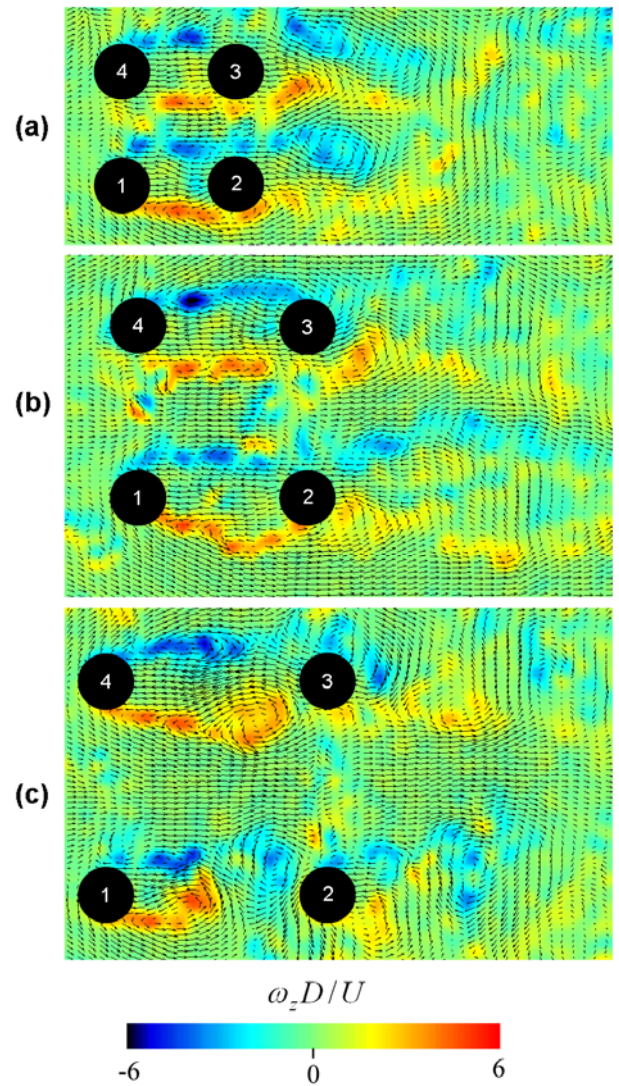


Figure 5. A representative snapshot of the instantaneous flow fields for the four-cylinder array at: (a)  $P/D = 2.0$ ; (b) 3.0; and (c) 4.0. Superimposed with colour-scaled contours of normalized spanwise vorticity.

Flow patterns play a major role in the behaviour of the flow-induced forces. The effects of varying the pitch ratio on the flow patterns around the four-cylinder array are depicted in Figure 5 in terms of instantaneous velocity and vorticity distributions measured with PIV. It can be clearly observed that depending on the value of  $P/D$ , the shear layers from the upstream cylinders

show different interference characteristics with the downstream cylinders: (i) shielding pattern at  $P/D = 2.0$ , where the shear layers engulf the downstream cylinders; (b) shear layer reattachment pattern at  $P/D = 3.0$ , where the shear layers reattach on the surface of the downstream cylinders; and (c) impinging regime at  $P/D = 4.0$ , where von-Karman vortices are periodically shed from the upper cylinders and impinge on the downstream cylinders. In other words, the instability mode of the shear layers from the upstream cylinders varies due to the presence of the downstream cylinders, that is, from anti-symmetric type (Karman vortices) to symmetric type (Kelvin-Helmholtz vortices) as  $P/D$  decreases.

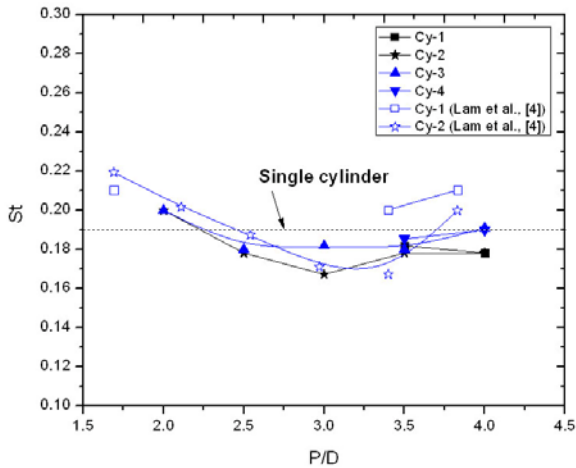


Figure 6. Variation of Strouhal number ( $St$ ) for vortex shedding frequency as a function of  $P/D$ .

Figure 6 shows the variation of  $St$  for the spectral peak (vortex shedding frequency) on each cylinder with respect to  $P/D$ . The results reported in [4] on Cy-1 and Cy-2 are also included for comparison purpose. In general, the agreement between the two data sets is good. Except for the case of very small pitch ratios ( $P/D \leq 3.5$ ) where no obvious vortex shedding is observed for the upstream cylinders (as confirmed by PIV results), the values of  $St$  are roughly equal to that of the single cylinder, i.e.,  $St \approx 0.19$ , with a relatively larger deviation in the small-to-moderate  $P/D$  range ( $P/D < 3.0$ ). In the large  $P/D$  range ( $P/D \geq 3.5$ ), by contrast, the data collapse perfectly, indicating the occurrence of vortex shedding from all cylinders, which can also be appreciated from the PIV results.

## Conclusions

The effects of variation in the centre-to-centre pitch on the vortex shedding patterns, hydrodynamic coefficients and vortex shedding frequencies of a four-cylinder array in in-line square configuration have been investigated experimentally. While the Reynolds number based on the cylinder diameter is fixed at  $Re = 1.1 \times 10^4$ , the centre-to-centre pitch ratio between adjacent cylinders is varied from  $P/D = 2.0$  to 4.0. It is clearly revealed that the flow pattern and hydrodynamic coefficients are strongly dependent on  $P/D$ . With the increase in  $P/D$ , the flow interference between the cylinders gradually changes from the shielding pattern at small  $P/D$ , to the shear layer reattachment pattern at moderate  $P/D$ , until the vortex impinging pattern at large  $P/D$ . As compared to the upstream cylinders, the mean drag coefficient for the downstream cylinders is consistently lower, but their RMS lift and drag coefficients are always higher (up to 6 ~ 7 times) within the measurement range. Also, the

spectra of the fluctuating lift forces and their corresponding spectral peaks (i.e., vortex shedding frequencies) for the upstream and downstream cylinders exhibit different characteristics with the change in  $P/D$ .

## Acknowledgments

The funding support from the Singapore National Research Foundation (NRF) through the Competitive Research Programme (CRP) through Project No. NRF-CRP5-2009-01 and Maritime and Port Authority (MPA) of Singapore on this project is gratefully acknowledged.

## References

- [1] Lam, K. & Fang, X., The effect of interference of four equispaced cylinders in cross flow on pressure and force coefficients, *J. Fluids Struct.*, **9**, 1995, 195-214.
- [2] Lam, K., Gong, W.Q. & So, R.M.C., Numerical simulation of cross-flow around four cylinders in an in-line square configuration, *J. Fluids Struct.*, **24**, 2008, 34-57.
- [3] Lam, K., Li, J.Y., Chan, K.T. & So, R.M.C., Flow pattern and velocity field distribution of cross-flow around four cylinders in a square configuration at a low Reynolds number, *J. Fluids Struct.*, **17**, 2003, 665-679.
- [4] Lam, K., Li, J.Y. & So, R.M.C., Force coefficients and Strouhal numbers of four cylinders in cross flow. *J. Fluids Struct.*, **18**, 2003, 305-324.
- [5] Lam, K., & Lo, S.C., A visualization study of cross-flow around four cylinders in a square configuration, *J. Fluids Struct.*, **6**, 1992, 109-131.
- [6] Lam, K. & Zou, L., Experimental and numerical study for the cross-flow around four cylinders in an in-line square configuration, *J. Mech. Sci. Tech.*, **21**, 2007, 1338-1343.
- [7] Lam, K. & Zou, L., Experimental study and large eddy simulation for the turbulent flow around four cylinders in an in-line square configuration, *Int. J. Heat Fluid Flow*, **30**, 2009, 276-285.
- [8] Lam, K. & Zou, L., Three-dimensional numerical simulations of cross-flow around four cylinders in an in-line square configuration, *J. Fluids Struct.*, **26**, 2010, 482-502.
- [9] Sayers, A.T., Flow interference between four equispaced cylinders when subjected to a cross flow, *J. Wind Eng. Ind. Aerodyn.*, **31**, 1988, 9-28.
- [10] Sayers, A.T., Vortex shedding from groups of three and four equispaced cylinders situated in a cross flow, *J. Wind Eng. Ind. Aerodyn.*, **34**, 1990, 213-221.
- [11] Sumner, D., Two circular cylinders in cross-flow: A review, *J. Fluids Struct.*, **26**, 2010, 849-899.
- [12] Sumner, D., Price, S.J. & Paidoussis, M.P., Flow-pattern identification for two staggered circular cylinders in cross-flow, *J. Fluid Mech.*, **411**, 2000, 263-303.
- [13] Zou, L., Lin, Y.-F. & Lam, K., Large-eddy simulation of flow around cylinder arrays at a subcritical Reynolds number, *J. Hydrodyn. Ser. B*, **20**, 2008, 403-413.
- [14] Zou, L., Lin, Y.-F. & Lu, H., Flow patterns and force characteristics of laminar flow past four cylinders in diamond arrangement, *J. Hydrodyn. Ser. B*, **23**, 2011, 55-64.